CT and MR Imaging of Gynecologic Emergencies[1]

Yuko Iraha, MD, PhD
Masahiro Okada, MD, PhD
Rin Iraha, MD
Kimei Azama, MD
Tsuneo Yamashiro, MD, PhD
Maho Tsubakimoto, MD
Yoichi Aoki, MD, PhD
Sadayuki Murayama, MD, PhD

SA-CME LEARNING OBJECTIVES

After completing this journal-based SA-CME activity, participants will be able to:

■ List the gynecologic diseases that manifest with acute abdominal pain and hemorrhage.

■ Recognize the CT and MR imaging features of acute gynecologic diseases.

■ Describe the importance of CT and MR imaging as part of the management strategy for patients with acute gynecologic diseases.

See www.rsna.org/education/search/RG.

Gynecologic emergencies include various diseases that result from adnexal and uterine disorders. Adnexal disorders may be classified into the following three categories: *(a)* disorders that cause hemorrhage (hemorrhagic ovarian cysts and ectopic pregnancies); *(b)* disorders related to adnexal tumors (adnexal torsion and rupture of ovarian tumors); and *(c)* disorders related to pelvic inflammatory disease, such as tubo-ovarian abscesses. Unusual adnexal torsion, such as massive ovarian edema, isolated fallopian tube torsion, and paraovarian cyst torsion, has also been described. Uterine disorders in gynecologic emergencies may be classified into two categories: *(a)* acute fibroid complications, including red degeneration of a uterine leiomyoma, torsion of subserosal myomas, and torsion of the uterus; and *(b)* causes of acute uterine bleeding, including retained products of conception and uterine arteriovenous malformations. Some gynecologic diseases are self-limited, while others cause infertility or life-threatening infection or bleeding if left untreated. Therefore, prompt and accurate diagnosis is important for appropriate life-saving treatment and for the preservation of fertility. The imaging findings are important when evaluating acute gynecologic diseases because the symptoms and physical examination findings are often nonspecific and limited. Ultrasonography is the first-line imaging modality; however, when a definitive diagnosis cannot be established, computed tomography (CT) and magnetic resonance (MR) imaging may narrow the differential diagnosis. Appropriate management requires radiologists to be familiar with the CT and MR imaging features of gynecologic emergencies. With respect to rare conditions, radiologists should take into account the representative findings presented in this article to increase diagnostic accuracy.

©RSNA, 2017 • *radiographics.rsna.org*

Introduction

Diagnosing gynecologic emergencies is challenging because symptoms and physical examination findings are often nonspecific. Imaging methods are useful for narrowing the differential diagnosis in patients with gynecologic emergencies. Computed tomography (CT) is available for emergency use and helps to exclude nongynecologic diseases, although patients will receive low-dose radiation exposure. CT can easily demonstrate pelvic lesions, and a presumptive diagnosis of gynecologic diseases can be made.

Currently, dual-energy CT has the potential for characterizing different materials on the basis of their elemental composition (1,2). Iodine mapping may be useful in differentiating the contrast agent from a hemorrhage, which increases the diagnostic accuracy for some acute gynecologic emergencies, such as hemorrhagic infarction in ovarian torsion. Dual-energy CT may also be used to characterize other materials, such as iron deposition in endometrial cysts. Dual-energy

TEACHING POINTS

- A twisted pedicle usually contains a thickened fallopian tube, which appears as a beak-like protrusion adjacent to the mass, continuous with the uterus. CT findings are commonly nonspecific, but careful reading and multiplanar reformation may help identify the thickened tube as amorphous or a tubular mass-like structure adjacent to the adnexal mass. It is important to know that a twisted pedicle does not always appear as a spiral configuration but occasionally appears like a solid-like component of the associated mass.

- The pathognomonic findings of MOE are multiple follicles situated at the periphery of the enlarged ovary, associated with severe stromal edema on US and T2-weighted MR images. In some cases, large mature follicles may also be observed.

- In isolated fallopian tube torsion, identification of an ipsilateral normal ovary is important.

- If an endometriotic cyst ruptures, the shape of the cyst may change, and the cyst fluid leakage may appear as loculated hyperintense fluid around the cyst on fat-saturated T1-weighted images.

- MR imaging typically shows an endometrial polypoid mass with heterogeneous signal intensity on T1- and T2-weighted images and variable enhancement on postcontrast images.

CT has the potential to increase contrast enhancement using virtual monochromatic images, which may contribute to the evaluation of disease severity in adnexal torsion or the detection of peritoneal inflammation. In addition, the clinical importance of dual-energy CT includes the replacement of a true nonenhanced scan with the use of a virtual nonenhanced scan, which reduces radiation exposure, especially in young patients.

Magnetic resonance (MR) imaging is superior to CT with respect to soft-tissue contrast resolution and gives more detailed information about pelvic lesions, which narrows the differential diagnosis of acute gynecologic diseases. MR imaging can assist with the diagnosis of hemorrhage by showing signal intensity changes within the lesions. Rare gynecologic conditions are often difficult to diagnose; however, comprehensive image interpretation can lead to an accurate diagnosis. Nevertheless, the imaging findings should be interpreted in association with the clinical presentation.

In this article, CT and MR imaging features and the clinical presentation of acute gynecologic conditions are described. Differential diagnoses, radiologic look-alikes, and the appropriate management of acute gynecologic diseases are also discussed.

Disorders of the Adnexa

Acute gynecologic diseases resulting from adnexal disorders are divided into three categories: *(a)* disorders causing acute hemorrhage from adnexal lesions, *(b)* disorders related to adnexal tumor, and *(c)* disorders related to pelvic inflammatory disease (PID) (Table 1).

Hemorrhage

Rupture of a hemorrhagic ovarian cyst or ectopic pregnancy may cause hemoperitoneum, and both have similar radiologic appearances. Although a patient with a positive pregnancy test should always be evaluated with ultrasonography (US) first, patients with ectopic pregnancies may be examined with CT for evaluation of a severe acute abdomen without prior US. Radiologists should know the imaging features and clinical manifestations of ruptured ovarian cysts and ectopic pregnancies.

MR imaging, which requires more time to perform than CT, is usually unnecessary or not indicated in patients with hemoperitoneum. This is because careful interpretation of the clinical presentation and US or CT findings can lead to the correct diagnosis; however, in ectopic pregnancies, MR imaging may be performed when US findings of the gestational sac location are unclear.

Hemorrhagic Ovarian Cyst.—A hemorrhagic ovarian cyst may be a physiologic event and a self-limited process that often involves a corpus luteum cyst rather than a follicular cyst. The increased vascularity of the ovary in the luteal phase may cause a cyst to rupture (3). Rupture of an ovarian cyst may be associated with sexual intercourse, exercise, trauma, and pregnancy, and it may involve the right ovary more frequently because the left ovary is protected by a cushion of sigmoid colon. Although cyst rupture may cause massive hemoperitoneum, most patients can be followed with conservative treatment unless they are in unstable condition (4).

The typical US findings of a hemorrhagic ovarian cyst include a low-level echogenic adnexal cyst with a lace-like internal appearance (5). The CT findings of a hemorrhagic ovarian cyst include a unilateral adnexal cyst with a high-attenuation area (>40 HU) within the cyst. Contrast material–enhanced CT helps delineate the cyst wall to show a corpus luteal cyst (Fig 1a).

After the cyst ruptures, hemoperitoneum can be observed as high-attenuation peritoneal free fluid (>30 HU). In some cases, extravasation of the contrast agent adjacent to the cyst may be observed on CT images (Fig 1b). The MR imaging appearance of a hemorrhagic cyst can be variable, depending on the age of the hemorrhage, with hyperintensity on both T1- and T2-weighted images or hyperintensity on T1-weighted images and hypointensity on T2-weighted images (6,7). The differential diagnosis based on the radiologic evaluation is an ectopic pregnancy.

Ectopic Pregnancy.—Ectopic pregnancies occur when the blastocyst implants outside the endometrium of the uterus. Ninety-five percent of

RadioGraphics

Table 1: Key Features of Acute Gynecologic Diseases Resulting from Adnexal Disorders

Acute Gynecologic Diseases	Occurrence and Clinical Manifestations	Appearance of Ipsilateral Ovary	Imaging Features		Differential Diagnosis
			CT	MR Imaging*	
Acute hemorrhage from adnexal lesions					
Hemorrhagic ovarian cyst	Common Occurs during luteal phase, antecedent intercourse Right-side dominant	Functional cyst	Adnexal cyst with high-attenuation area Hemoperitoneum if ruptured	Usually not indicated	Ectopic pregnancy
Ectopic (tubal) pregnancy	Common Serum β-hCG positive	Normal	Adnexal cystic mass separated from normal ovary	Usually not indicated	Hemorrhagic ovarian cyst
Adnexal tumor–related disorders					
Ovarian torsion	Uncommon Sharp localized right or left lower abdominal pain Ipsilateral pelvic mass	Obscured or enlarged†	Usually cystic tumor > 5 cm Beak-like protrusion Absent enhancement of an adnexal mass	Beak-like protrusion (T2WI, DWI) Wall thickening of the mass (T2WI, DWI) Absent enhancement of the mass (CE FS T1WI) Cyst wall or internal hemorrhage (FS T1WI)	Torsion of a subserosal myoma Rupture of an ovarian tumor
MOE (torsion of normal ovary)	Rare Intermittent/recurrent pain Occurs during pregnancy or ovulation induction or in perimenarchal girls	Enlarged	Nonspecific Solid-like adnexal mass Few large follicles as functional cysts	Enlarged ovary with stromal edema and peripherally located small follicles (T2WI) A few large follicles as functional cysts (T2WI) Internal hemorrhage (FS T1WI)	Ovarian tumor
Isolated fallopian tube torsion	Extremely rare Clinical features are indistinguishable from those of ovarian torsion Sharp localized right or left lower abdominal pain Ipsilateral pelvic mass	Normal	Adnexal cystic mass or tubal dilatation	Adnexal cystic mass or tubal dilatation (T2WI) Whirlpool sign of twisted pedicle (T2WI)	Ovarian torsion
Rupture of cystic teratoma	Rare Large pelvic mass	Obscured	Mature cystic teratoma with distorted shape Fatty implants within peritoneum	Mature cystic teratoma with distorted shape (T1WI) Fatty implants within peritoneum (T1WI) Peritoneal thickening and stranding (CE FS T1WI)	Ovarian torsion
Rupture of endometriotic cyst	Rare Abdominal pain without apparent laterality Elevated serum tumor markers	Obscured	Nonspecific Cystic mass with slightly attenuated content Loculated ascites around the mass	Endometriotic cyst with distorted shape (T1WI, T2WI) T1 hyperintense fluid around the cyst (FS T1WI) Peritoneal thickening and stranding (CE FS T1WI)	Ovarian torsion TOA Ovarian malignancy
PID-related disorders					
TOA	Common Fever Vaginal discharge STD Iatrogenic	Obscured	Adnexal thick-walled complex cystic mass with tubal structure and intense enhancement Surrounding peritoneal thickening and stranding	Adnexal thick-walled complex mass with tubal structure and intense enhancement (T2WI, CE FS T1WI) Surrounding severe peritoneal inflammation (CE FS T1WI) Hyperintense content at DWI	Ovarian malignancy

Note.—CE = contrast-enhanced, DWI = diffusion-weighted imaging, FS = fat-saturated, hCG = human chorionic gonadotropin, MOE = massive ovarian edema, STD = sexually transmitted disease, TOA = tubo-ovarian abscess, T1WI = T1-weighted imaging, T2WI = T2-weighted imaging.
*Parentheses list useful imaging sequences.
†Secondary MOE.

a.   b.
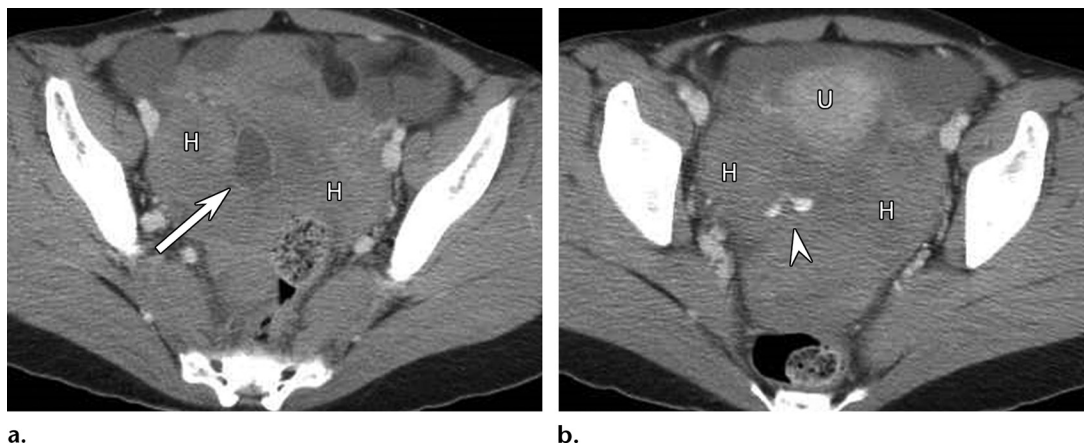
Figure 1. Ruptured hemorrhagic ovarian cyst in a 30-year-old woman. *H* = hemoperitoneum. **(a)** Axial contrast-enhanced CT image shows a right adnexal cystic mass (arrow). **(b)** Contrast-enhanced CT image (obtained caudal to **a)** shows extravasation (arrowhead) of contrast medium. The clinical presentation was lower abdominal pain with transient syncope at her menstrual midcycle. The symptoms resolved with conservative treatment. *U* = uterus.

Figure 2. Ruptured tubal ectopic pregnancy in a 33-year-old woman. Contrast-enhanced CT image shows a left adnexal cystic mass (arrow) with surrounding hemoperitoneum *(H)*. *U* = uterus.
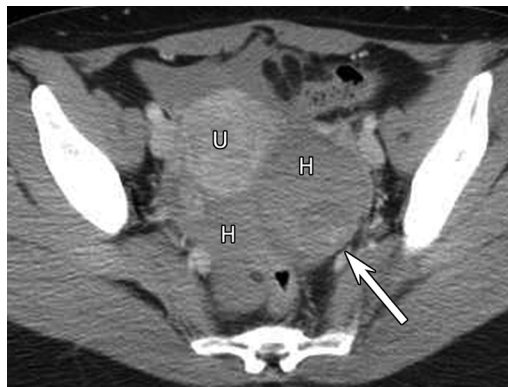
ectopic pregnancies are tubal, and most commonly occur in the ampulla of the fallopian tube. The characteristic imaging finding of a tubal ectopic pregnancy is an adnexal cystic sac-like structure that is separate from an ipsilateral normal ovary, representing a gestational sac (8). The CT findings include an adnexal cystic mass with some degree of peripheral enhancement at contrast-enhanced CT (Fig 2). A hemoperitoneum can be observed if the ectopic gestation ruptures. MR imaging features include a hematosalpinx, a hemorrhagic or heterogeneous mass, bloody ascites, tubal dilatation, and tubal wall enhancement.

Adnexal Torsion

Adnexal torsion can involve the ovary, fallopian tube, or both. Combined ovarian and tubal torsion is the most common finding in patients with adnexal torsion and is usually associated with an ovarian mass. Torsion of a normal ovary is a rare entity that predominantly occurs in perimenarchal girls or during pregnancy, and it may cause massive ovarian edema (MOE). Isolated fallopian tube torsion is extremely rare and is thought to be associated with tubal diseases or conditions. Paraovarian cysts rarely undergo torsion.

Ovarian Torsion.—Ovarian torsion is a well-known gynecologic emergency that is usually caused by the twisting of the ovary and fallopian tube. Ovarian torsion can occur in women of all ages, but the highest prevalence is among women

of reproductive age (9,10). Ovarian torsion is frequently associated with benign ovarian masses, such as mature cystic teratomas that are greater than 5 cm in diameter (Fig 3).

In contrast, malignant ovarian tumors and endometriotic cysts are less likely to cause ovarian torsion due to adhesions. Traditional symptoms of ovarian torsion include the sudden onset of sharp lower quadrant pain with nausea and vomiting; however, intermittent or gradually increasing pain attacks have been observed in some cases and are thought to represent episodes of torsion and detorsion (11).

CT and MR imaging features of ovarian torsion are classified into direct and indirect findings of torsion. The former indicates a twisted structure of the adnexa or morphologic change due to torsion. The latter indicates secondary edematous or ischemic changes of an affected ovary and related mass due to a disruption in blood flow (9–15).

One direct finding of torsion is a twisted pedicle, which is considered pathognomonic of torsion, as well as fallopian tube thickening (12). Another direct finding of torsion is ipsilateral uterine deviation due to a shortened adnexal

a.   b.
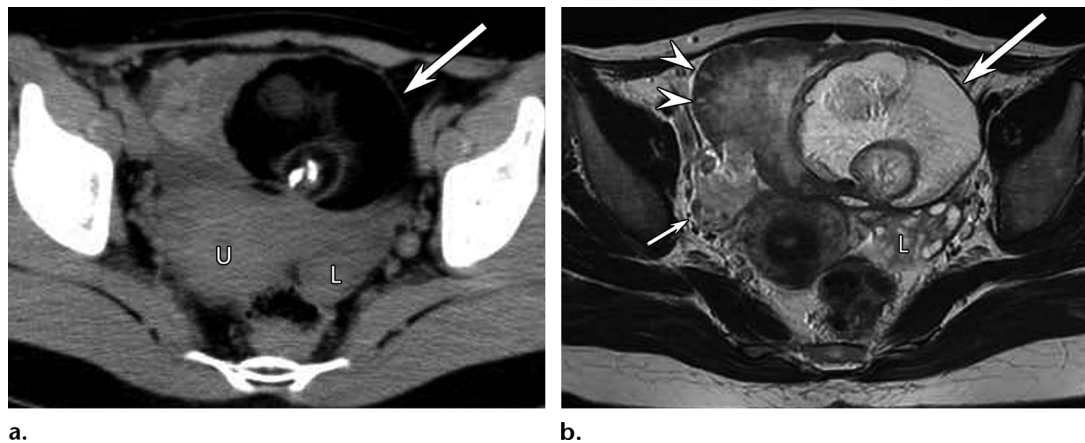
Figure 3.   Torsion of a mature cystic teratoma in a 31-year-old woman. *L* = left ovary. **(a)** Axial contrast-enhanced CT image shows a fat-containing tumor (arrow) with foci of calcifications, which are indicative of a cystic teratoma. *U* = uterus. **(b)** Axial T2-weighted MR image shows a relatively hypointense solid-like mass (arrowheads) adjacent to the cystic teratoma (large arrow) with peripherally located small cysts, indicative of a secondary MOE with hemorrhage. A beak-like protrusion (small arrow) of a twisted pedicle and ipsilateral uterine deviation are also shown.

ligament, although this finding is not specific. A twisted pedicle usually contains a thickened fallopian tube, which appears as a beak-like protrusion adjacent to the mass, continuous with the uterus (Fig 4). CT findings are commonly nonspecific, but careful reading and reformation may help identify the thickened tube as an amorphous or tubular mass-like structure adjacent to the adnexal mass. It is important to know that a twisted pedicle does not always appear as a spiral configuration but occasionally appears like a solid-like component of the associated mass (Fig 5). MR images may depict a twisted pedicle more clearly, but the signal intensity of a twisted pedicle depends on the degree of edema or ischemia, which is described in the following paragraph.

Secondary edematous or ischemic changes of ovarian torsion progress in stages. Ovarian torsion initially causes interruption of venous and lymphatic outflow and leads to edematous changes and congestion, which are represented as an enlarged edematous ovary, fallopian tube thickening, and/or smooth wall thickening of the adnexal mass (Figs 3, 4). As severe venous congestion persists, arterial blood flow becomes interrupted. Ischemia and hemorrhagic infarction may occur as minimal or absent enhancement of the mass and hemorrhage in the wall of the cystic mass or within the mass. Hemorrhage and absence of enhancement may also be observed in a thickened fallopian tube. Edematous ovaries can be identified on T2-weighted images as hyperintense or intermittently intense signals with peripherally located small follicles (Fig 3b), which are described in the following section regarding MOEs.

Without hemorrhage, the thickened fallopian tube may appear as low signal intensity on T1-weighted images and high signal intensity on T2-weighted images. When hemorrhagic infarction occurs, the wall of the cystic mass, the inside of the mass, or the thickened fallopian tube may appear hyperintense on fat-saturated T1-weighted images (Fig 4b). At CT, hemorrhage may also appear as a high-attenuation area, but fat-saturated T1-weighted images show hemorrhage more clearly. Minimal or absent enhancement of the mass can be confirmed at gadolinium-enhanced subtraction MR imaging, even if the mass appears hyperintense due to hemorrhage. At contrast-enhanced CT, the abnormal enhancement can be perceived, but it is difficult to discern compared with that at subtraction MR imaging.

Recent studies have reported the usefulness of diffusion-weighted MR images in the evaluation of ovarian torsion (14–17). Diffusion-weighted images may show abnormal signal intensity in the thickened fallopian tube and in the wall of the cystic ovarian mass. Hemorrhagic infarction may be associated with high signal intensity on diffusion-weighted images (Fig 4c).

Massive Ovarian Edema.—MOE is a rare tumor-like entity that appears as a solid enlargement of the ovary and is associated with severe stromal edema. MOE can occur primarily in a normal ovary without neoplastic change or secondarily in a diseased ovary (18). Secondary MOE is often observed simultaneously with ovarian torsion associated with benign ovarian masses, as previously described. Perimenarchal girls, women undergoing ovulation induction, and pregnant women are commonly affected, for those groups have a tendency toward developing functional cysts or have easily mobile adnexa. Partial recurrent torsion of a normal ovary is thought to cause MOE due to interference with
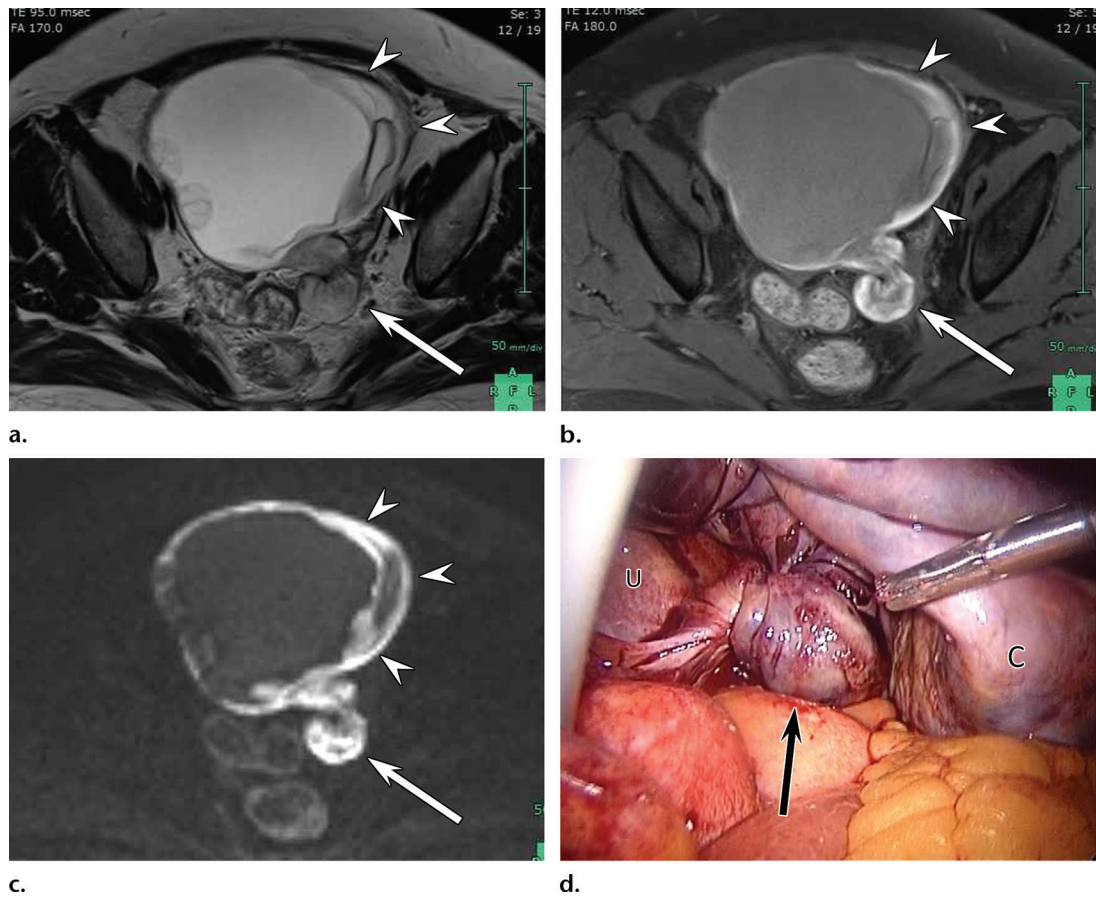
Figure 4. Torsion of a cystic mass with hemorrhagic infarction in a 66-year-old woman. **(a)** Axial T2-weighted MR image shows a cystic mass with a thickened wall (arrowheads). At pathologic analysis, the cystic lesion was indeterminate. **(b)** Axial T1-weighted MR image shows high signal intensity of the thickened wall of the cyst (arrowheads) and a thickened left fallopian tube (arrow in **a** and **b**). **(c)** Axial diffusion-weighted MR image shows high signal intensity of the thickened wall (arrowheads) and the fallopian tube (arrow). An apparent diffusion coefficient (ADC) map showed significantly decreased ADC for these areas (not shown). **(d)** Intraoperative photograph shows a twisted and thickened fallopian tube (arrow). Note that the twisted pedicle appears as a tight knot. *C* = cystic mass, *U* = uterus.
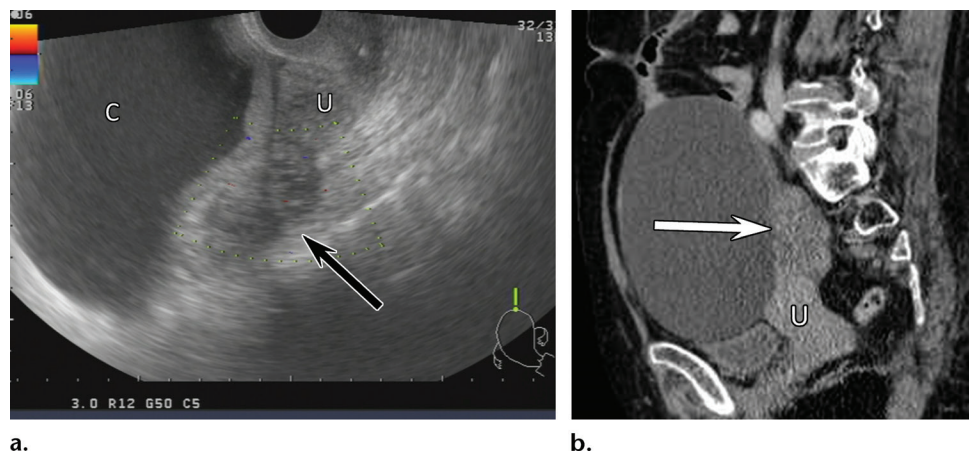
Figure 5. Torsion of a cystic mass with hemorrhagic infarction in a 65-year-old woman. **(a)** Transvaginal US image of the right adnexa shows a heterogeneous solid-like mass (arrow) closely attached to a large cystic mass *(C)* and the uterus *(U)*. Color Doppler US image showed minimal internal vascularity of the mass. **(b)** Sagittal contrast-enhanced CT image shows a large cystic mass with a solid-like component (arrow) posterior to the cyst and superior to the uterus *(U)*, corresponding to the solid-like mass on the US image (shown in **a**). The solid-like component was confirmed surgically to be severe hemorrhage and necrosis, indicative of a thickened fallopian tube with hemorrhagic infarction. At pathologic analysis, the cystic lesion was indeterminate.

a.   b.
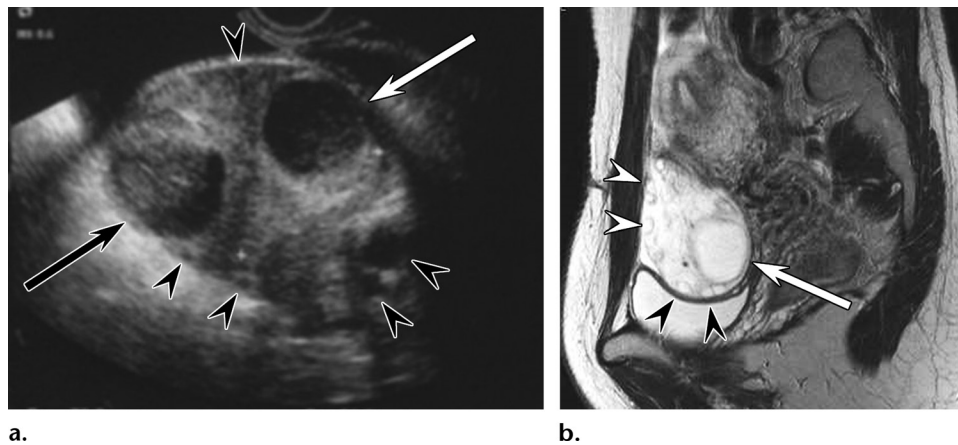
Figure 6. MOE in a 29-year-old woman during ovulation induction. **(a)** Transvaginal US image of the left adnexa shows a heterogeneous enlarged ovary with peripherally located small follicles (arrowheads). Mature follicles (arrows), likely due to ovulation induction, are also shown. **(b)** Sagittal T2-weighted MR image shows multiple small follicles (arrowheads) situated at the periphery of the enlarged ovary. A large mature follicle (arrow) is also shown. Surgical detorsion was successfully performed and confirmed the diagnosis.

venous and lymphatic drainage (19). A prompt and accurate diagnosis of MOE is important for preserving the ovary and avoiding an unnecessary salpingo-oophorectomy.

The pathognomonic findings of MOE are multiple follicles situated at the periphery of the enlarged ovary, associated with severe stromal edema on US and T2-weighted MR images (9–11,20). In some cases, large mature follicles may also be observed (Fig 6). The common gray-scale US findings include engorgement of the ovary with slight central hyperechogenicity (indicative of edema), hemorrhage, and multiple peripheral cysts (consistent with follicles). The color Doppler US findings are variable and depend on the degree of vascular compromise. MR imaging findings include solid tumor-like enlargement of the ovary and hyperintensity on T2-weighted images, with multiple peripheral small cysts.

Hemorrhage within the ovarian stroma may be observed as hyperintensity on T1-weighted MR images and hypointensity on T2-weighted images, as shown in Figure 3b (21). Contrast enhancement of the enlarged ovarian stroma and cyst walls may remain in cases of partial ovarian torsion. CT findings are considered nonspecific, and an enlarged ovary may appear as a solid tumor-like mass. Therefore, in combination with US or additional MR imaging, careful image interpretation is important. After the diagnosis of MOE is considered, laparoscopic detorsion of the ovary and wedge resection with frozen section analysis facilitate conservation of the ovaries (18,22,23).

Isolated Fallopian Tube Torsion.—Isolated fallopian tube torsion is extremely rare, while adnexal torsion that includes the ovary and fal-

lopian tube is relatively common among gynecologic emergencies (24–26). Isolated fallopian tube torsion most commonly occurs during the reproductive ages and rarely occurs during postmenopause. The predisposing factors for isolated fallopian tube torsion are tubal conditions, including hydrosalpinx, tubal ligation, and tubal or paratubal masses. Clinical symptoms are indistinguishable from those of ovarian torsion (ie, a sudden onset of lower quadrant pain with nausea and vomiting).

A preoperative diagnosis is difficult because of the rarity of the condition and its nonspecific clinical presentation; however, the rate of preoperative diagnosis increases based on radiographic findings (27,28). US findings include tubal dilatation with thickened echogenic walls and internal debris or an associated cystic mass separate from the ovary (29). CT images may show an adnexal cystic structure separate from the ovary, which is easily depicted using multiplanar reformation. MR imaging allows easy distinction of a normal ovary from a cystic mass, and the whirlpool sign of a twisted pedicle may be observed on T2-weighted MR images (Figs 7, 8).
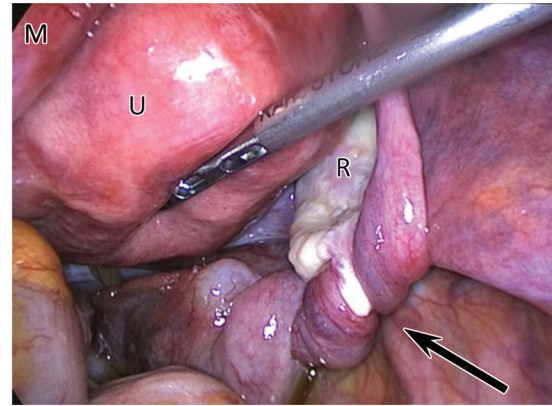
In isolated fallopian tube torsion, identification of an ipsilateral normal ovary is important. Contrast-enhanced subtraction T1-weighted MR images help identify the vascularity of the affected organs. Although necrosis of the fallopian tube may occur, ischemic change of the adjacent ovary does not occur due to the spared suspensory ligament with conserved ovarian vascular supply (30). The vascular supply for an associated tubal or paraovarian mass may also be conserved based on the dual blood supply to the adnexa from ovarian and uterine vessels. There may be a tendency for more twists compared with ovarian torsion because of the long axis (Figs 7, 8).
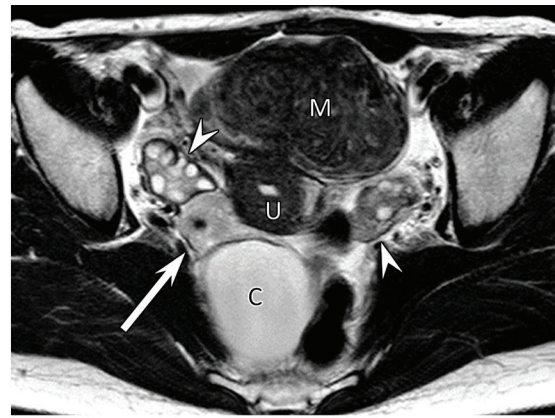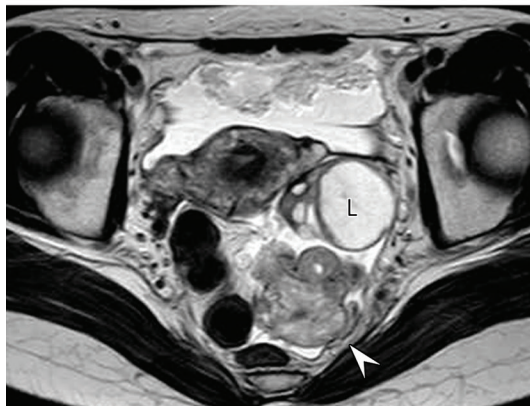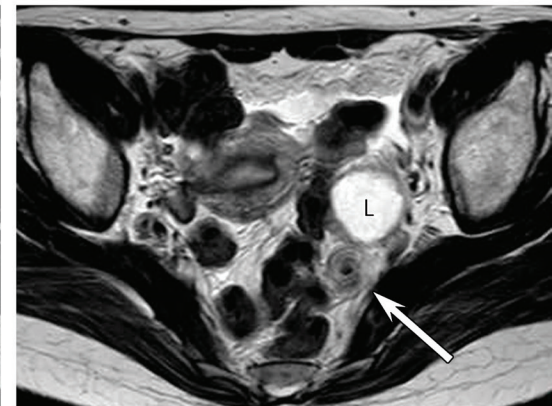
7a.
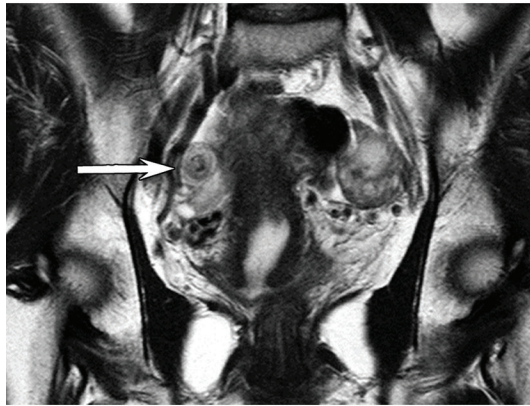
7b.

7c.

8a.

8b.

Figures 7, 8.   **(7)** Isolated fallopian tube torsion in a 38-year-old woman. *M* = myoma, *U* = uterus. **(a)** Axial T2-weighted MR image shows a cystic mass *(C)* posterior to the uterus and a thickened right fallopian tube (arrow) between the uterus and the cystic mass. The ovaries (arrowheads) are normal bilaterally. Note that the surface of the left side of the right ovary is extended to the right fallopian tube. **(b)** Coronal T2-weighted MR image shows a whirlpool sign (arrow) of the right fallopian tube. **(c)** Intraoperative photograph shows a twisted right fallopian tube (arrow). The ipsilateral ovary is normal in appearance, but the surface of the ovary is extended to the twisted fallopian tube, which corresponds to the imaging findings in **a**. A paratubal cyst was located near the fimbria (not shown). The right fallopian tube was twisted four times. Pathologic analysis confirmed serous cystadenoma without hemorrhage or necrosis. *R* = right ovary. **(8)** Isolated fallopian tube torsion in a 37-year-old woman. *L* = left ovary. **(a)** Axial T2-weighted MR image shows a solid mass (arrowhead) in the cul-de-sac separate from the left ovary. **(b)** Axial T2-weighted MR image (obtained cranial to **a**) shows a whirlpool structure (arrow) between the uterus and the mass. The left fallopian tube was twisted four times at the surgical excision. The solid mass was located within the left fimbria. Pathologic analysis confirmed a female adnexal tumor of probable Wolffian origin (FATWO).

Paraovarian Cyst Torsion.—Paraovarian or paratubal cysts are located in the broad ligament between the ovary and fallopian tube and constitute approximately 10% of all adnexal masses. Most patients with paraovarian cysts are asymptomatic. Paraovarian cysts rarely undergo torsion, but

Figure 9. Torsion of a paraovarian cyst in a 20-year-old woman. **(a)** Axial T2-weighted MR image shows a cystic mass (arrow) posterior to the uterus. A small cyst adjacent to the cystic mass is indicative of a left ovary (arrowhead). **(b)** Axial contrast-enhanced T1-weighted MR image with fat saturation shows absence of enhancement of the cystic mass (arrow). The thickened left fallopian tube is shown with slight enhancement (arrowhead). **(c)** Intraoperative photograph shows torsion of a paraovarian cyst (arrow). The left ovary *(L)* and fallopian tube are slightly involved and congested (arrowheads). The congestion disappeared after detorsion, and the left adnexa was preserved. Pathologic analysis confirmed serous papillary cystadenoma with internal hemorrhage. *R* = right ovary, *U* = uterus.
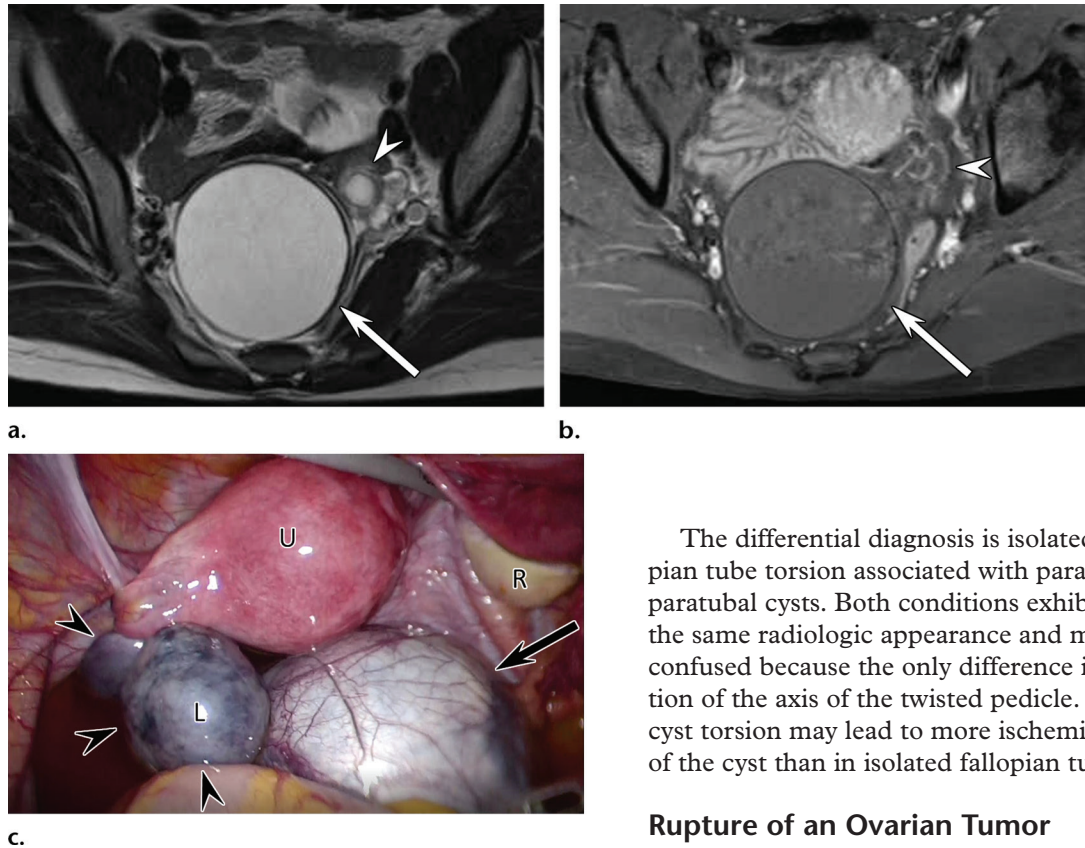
they have been reported (31,32). Although the rate of occurrence of cysts in children is assumed to be low, the torsion rate of paraovarian cysts in children is known to be higher than in adults. Torsion of paraovarian cysts may be accompanied by tubo-ovarian torsion, but torsion of only paraovarian cysts has been reported.

Although both US and MR imaging are useful diagnostic tools, MR imaging is more definitive. A paraovarian cyst is suggested when a simple unilocular cyst separates from the ipsilateral ovary and is noted at US. MR imaging of paraovarian cysts usually shows a well-defined homogeneous cystic structure separate from the ovary with high signal intensity on T2-weighted images and low signal intensity on T1-weighted images (Fig 9a); however, the internal signals of the cyst may change to a slightly high signal intensity on T1-weighted images if hemorrhage occurs due to torsion. A beak-like protrusion can be detected adjacent to the cyst if accompanied by tubo-ovarian torsion, corresponding to a twisted pedicle and fallopian tube thickening (Fig 9b, 9c).

The differential diagnosis is isolated fallopian tube torsion associated with paraovarian or paratubal cysts. Both conditions exhibit nearly the same radiologic appearance and may often be confused because the only difference is localization of the axis of the twisted pedicle. Paraovarian cyst torsion may lead to more ischemic changes of the cyst than in isolated fallopian tube torsion.

Rupture of an Ovarian Tumor

Rupture of an Ovarian Cystic Teratoma.—Rupture of an ovarian mature cystic teratoma may cause an acute abdomen. Rupture may result from torsion with infarction of the tumor, trauma, infection, prolonged pressure from pregnancy or during labor, a malignant change, or a rapid increase in the size of the mass (6,33). Spontaneous rupture of a mature cystic teratoma is thought to be rare due to its thick capsule. Ayhan et al (34) reported that the most common complication of mature cystic teratomas was torsion (4.9%), followed by rupture (2.5%), in the analysis of 501 patients with mature cystic teratoma. Sudden rupture leads to acute abdominal pain secondary to severe chemical peritonitis due to irritation from leakage of the cyst fluid, whereas chronic leakage leads to progressive abdominal distention. The cyst fluid includes sebaceous material, hair epithelial cells, and digestive enzymes.

Radiologic features are associated with mature cystic teratomas. CT scans commonly demonstrate a cystic mass containing large amounts of fat and solid mural nodules with calcifications. MR imaging can also demonstrate fat components within the tumor with a combination of T1-weighted

Figure 10. Rupture of a mature cystic teratoma in a 45-year-old woman. **(a, b)** Axial contrast-enhanced CT image **(a)** and axial T1-weighted MR image **(b)** show a fat-containing cystic tumor (arrow) and multiple fatty implants (arrowheads) within the peritoneal cavity. **(c)** Axial contrast-enhanced T1-weighted MR image with fat saturation depicts peritoneal stranding (arrowheads). Levels of the serum tumor markers CA-125 and CA-19-9 were elevated, but the squamous cell carcinoma antigen (SCC) level was within the normal range. Pathologic analysis confirmed a mature cystic teratoma without malignant change.
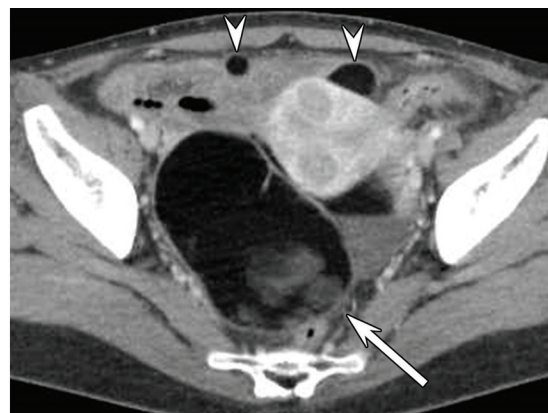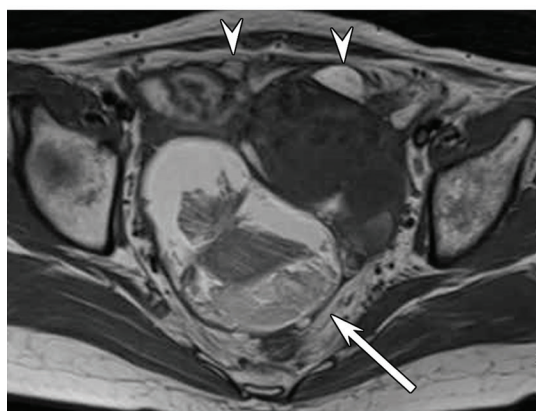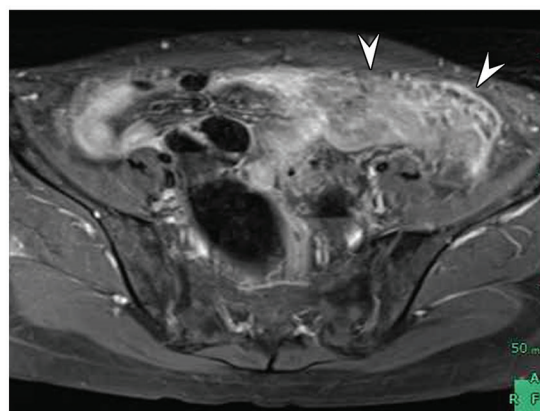
images and fat-saturated T1-weighted images. If ruptured, the appearance of the mass may change with a distorted shape and irregular wall thickening. The cyst fluid leakage may appear as a fatty implant within the peritoneal cavity, which can be detected as a well-demarcated ovoid or fusiform shape with a low-attenuation area on CT images (Fig 10a) and high signal intensity on T1-weighted MR images (Fig 10b). Subsequent peritonitis can be easily detected as peritoneal thickening and stranding on contrast-enhanced fat-saturated T1-weighted images (Fig 10c).

Chemical peritonitis may be mistaken for carcinomatosis; however, malignant transformation should be ruled out if a cystic teratoma is ruptured (35).
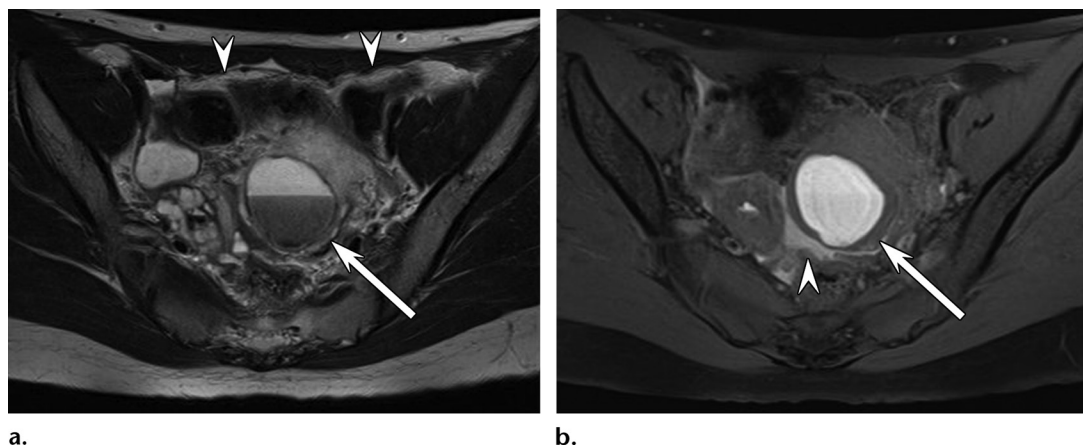
Rupture of an Ovarian Endometriotic Cyst.—
Spontaneous rupture of an endometriotic cyst is a rare complication of an ovarian endometrioma that causes severe acute abdominal pain due to chemical peritonitis from the leakage of old blood. A ruptured endometriotic cyst is associated with pregnancy and the large size of the cyst (36,37). In nonpregnant patients, rupture commonly occurs at menstruation due to an increase in internal pressure. Levels of serum tumor markers are often elevated due to the diffusion of

cyst fluid that is rich with CA-125 and CA-19-9 molecules through the peritoneal surface into the circulation. This phenomenon is often reported with signs of peritonitis, thus causing possible misinterpretation as a malignancy. The tumor marker levels may decrease if benign (38).

Ovarian endometriomas are typically demonstrated as hyperintense cystic masses on T1-weighted images with shading on T2-weighted images. The specific sign is a T2 dark spot, which is defined as a discrete well-defined markedly hypointense focus within the adnexal cystic mass on T2-weighted images (39). If an endometriotic cyst ruptures, the shape of the cyst may change, and the cyst fluid leakage may appear as loculated hyperintense fluid around the cyst on fat-saturated T1-weighted images (Fig 11) (6). The CT findings of a ruptured endometriotic cyst are a cystic mass with a slightly high-attenuation content and loculated ascites around the mass; however, these findings are somewhat nonspecific, and it can be difficult to exclude ovarian torsion.

Subsequent peritonitis can be easily detected as peritoneal thickening and stranding on contrast-enhanced fat-saturated T1-weighted images. The differential diagnosis includes ovarian torsion, malignancy, and tubo-ovarian abscess

a. **b.**

Figure 11. Rupture of an ovarian endometriotic cyst in a 26-year-old woman during menstruation. **(a)** Axial T2-weighted MR image shows a left adnexal cystic mass (arrow) with a fluid-fluid level and marked shading. Slight peritoneal stranding is shown anteriorly (arrowheads). **(b)** Axial T1-weighted MR image with fat saturation shows hyperintense ascites (arrowhead) around the endometriotic cyst (arrow). Note the slightly distorted shape of the mass. Levels of the serum tumor markers CA-125 and CA-19-9 were elevated above the normal range.

(TOA). Torsion of an endometriotic cyst rarely occurs because of adhesions; therefore, severe abdominal pain and the typical findings of ovarian endometriotic cysts are indicative of rupture rather than torsion, especially with elevated levels of serum CA-125 and CA-19-9.

Pelvic Inflammatory Disease

PID is an infection of the upper female genital tract, including the endometrium, fallopian tubes, and ovaries. Sexually transmitted diseases and iatrogenic causes are well described. Typical symptoms of PID include lower abdominal pain, vaginal discharge, fever, and dyspareunia. PID usually affects young women of reproductive ages and may cause long-term complications, including infertility, ectopic pregnancy, and chronic pelvic pain, if left untreated.

Tubo-ovarian Abscess.—A TOA is a late complication of PID and occurs in approximately one-third of patients hospitalized for PID (40). TOAs are usually treated with aggressive medication or surgical resection, and rupture of an abscess may result in sepsis.

The US findings of a TOA include an adnexal mass with solid, cystic, or complex components. The CT and MR imaging features of a TOA are a uni- or multilocular adnexal mass with thick and intensely enhancing walls. The common CT finding is a low-attenuation complex adnexal mass with a thickened wall and internal septa (Fig 12a). The ipsilateral mesosalpinx is frequently thickened and displaced anteriorly.

The content of the abscess usually appears as low signal intensity on T1-weighted images and heterogeneous high signal intensity on T2-weighted images, but the signal intensity of the

content can vary depending on the viscosity or protein concentration. A hyperintense rim on the T1-weighted image along the inner layer of the thickened wall represents granulation tissue with microscopic bleeding (40,41). A pyosalpinx is often observed as a fluid-filled dilated tortuous structure with wall thickening around the mass on T2-weighted images (Fig 12b). A thickened and intensely enhanced wall of the mass, peritoneal stranding, and enhancement of the adjacent peritoneum or intestine may be frequently observed on contrast-enhanced fat-saturated T1-weighted images (Fig 12c) (42). Recently, it has been reported that the content of an abscess is usually hyperintense on diffusion-weighted images due to true restricted diffusion (43) (Fig 12d).

Disorders of the Uterus

Acute gynecologic diseases that result from uterine disorders are divided into two categories: acute fibroid complications and acute uterine bleeding (Table 2). The latter category is focused on the conditions that may cause delayed postpartum hemorrhage (PPH).

Acute Fibroid Complications

Red Degeneration of a Leiomyoma.—Red degeneration of a uterine leiomyoma, which consists of hemorrhagic infarction of the leiomyoma, may cause acute abdominal pain. This condition occurs secondary to venous thrombosis within the periphery of the lesion (44). Red degeneration occurs most often during pregnancy and is also associated with oral contraceptive use (44,45). The US findings of a leiomyoma are a well-defined solid mass; however, degeneration may be more complex with cystic changes or heterogeneity. The Doppler US

Table 2: Key Features of Acute Gynecologic Diseases That Result from Uterine Disorders

Acute Gyneco-logic Diseases	Occurrence and Clinical Features	Appearance of Bilateral Ovaries	Imaging Features		Differential Diagnosis
			CT	MR Imaging*	
Acute fibroid complications					
Red degeneration of myoma	Uncommon Occurs during pregnancy	Normal	Nonspecific Not indicated due to pregnancy	Peripheral or diffuse hyperintensity on T1WI Hypointense rim on T2WI	Pregnancy-related conditions
Torsion of a subserosal leiomyoma	Uncommon Pelvic mass Abdominal pain toward the mass	Normal	Nonenhanced pelvic mass connecting to the normally enhanced uterus No protrusion	Pedunculated sub-serosal leiomyoma (T2WI) Twisted pedicle may be thin	Ovarian torsion Ovarian tumor Degenerated myoma
Torsion of the uterus†	Extremely rare Lower abdominal pain Large pelvic mass	Normal but extend-ed‡	Whorled struc-ture of the uterus	Large fundal myoma Whorled structure of the uterine corpus (isthmus)	Torsion of subserosal myoma
Acute uterine bleeding					
RPOC	Common Secondary PPH	Normal	Hypo- or hyper-vascular endo-metrial mass at CE CT	Endometrial polypoid mass with heteroge-neous signal intensity, usually low on T1WI and high on T2WI Variable enhancement on postcontrast im-ages	Uterine AVM
Uterine AVM	Rare Secondary PPH	Normal	Vascular lesion with myometri-al involvement Early venous return at CE CT	Vascular lesion with myometrial involve-ment Flow void within the mass (T1WI, T2WI)	RPOC Pseudoaneu-rysm

Note.—AVM = arteriovenous malformation, CE = contrast-enhanced, RPOC = retained products of concep-tion, T1WI = T1-weighted image, T2WI = T2-weighted image.
*Parentheses list useful imaging sequences.
†Fibroid is the most common predisposing factor in a nongravid uterus.
‡May be involved in twisted pedicle.

findings of a leiomyoma with red degeneration may show decreased or absent flow. MR imaging is helpful for evaluating acute complications of leiomyomas. Leiomyomas with red degeneration may appear as peripheral or diffuse hyperinten-sity on T1-weighted images and variable signal intensity with or without a hypointense rim on T2-weighted images (Fig 13). The signal intensity characteristics of the rim are explained as an effect of abundant intracellular methemoglobin in the obstructed vessels (46). The entire lesion shows no

enhancement, although gadolinium is not admin-istered to pregnant patients.

Torsion of a Subserosal Leiomyoma.—Acute torsion of a subserosal uterine leiomyoma is rare. The differential diagnosis includes ovarian torsion, ovarian tumor, large leiomyoma with massive ne-crotic infarction, or uterine torsion (3,47). CT and MR imaging features show a pelvic mass without enhancement connecting to the normally en-hanced uterus. The ovaries appear normal bilater-
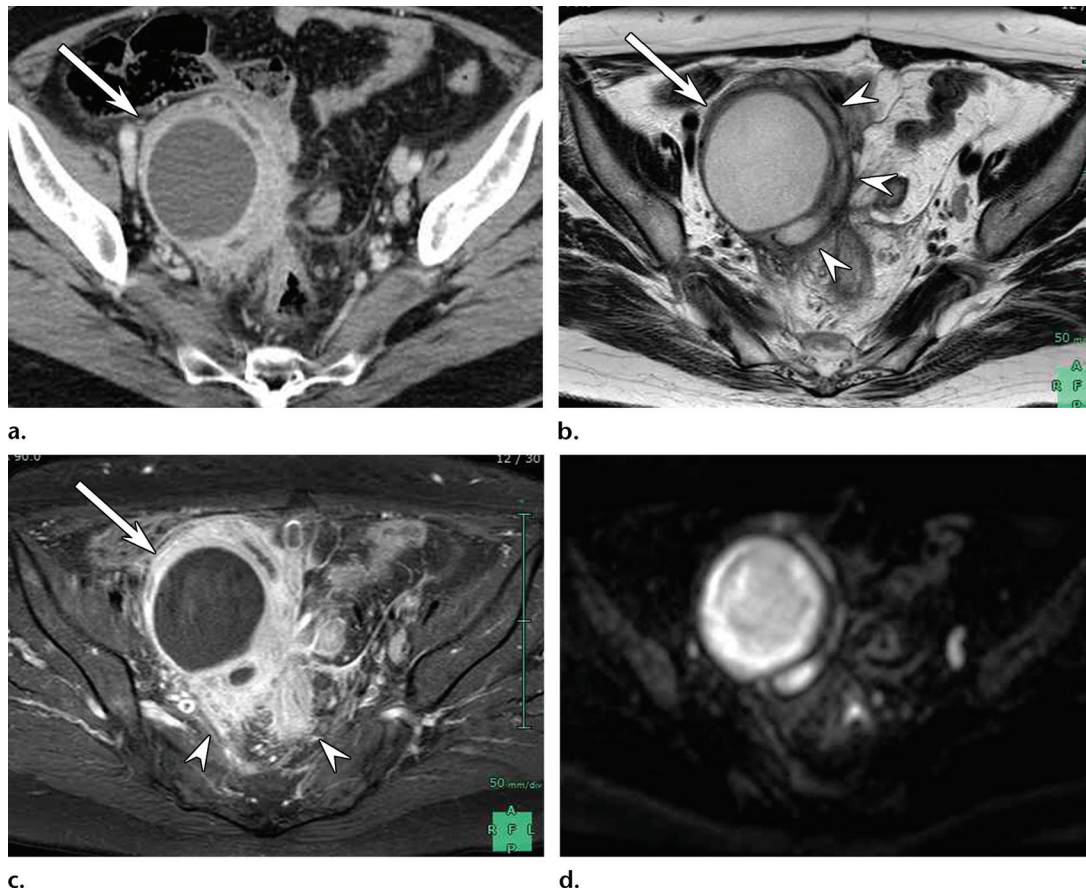
Figure 12.   TOA in a 65-year-old woman 6 months after dilation and curettage. **(a)** Axial contrast-enhanced CT image shows a right adnexal cystic mass (arrow) with an enhanced thickened wall. **(b)** Axial T2-weighted MR image reveals a pyosalpinx (arrowheads) around the cystic mass (arrow). **(c)** Axial contrast-enhanced T1-weighted MR image with fat saturation shows a cystic mass with an enhanced thickened wall (arrow) and severe inflammation around the cyst (arrowheads). **(d)** Diffusion-weighted MR image shows hyperintense fluid within the mass, indicative of pus collection.
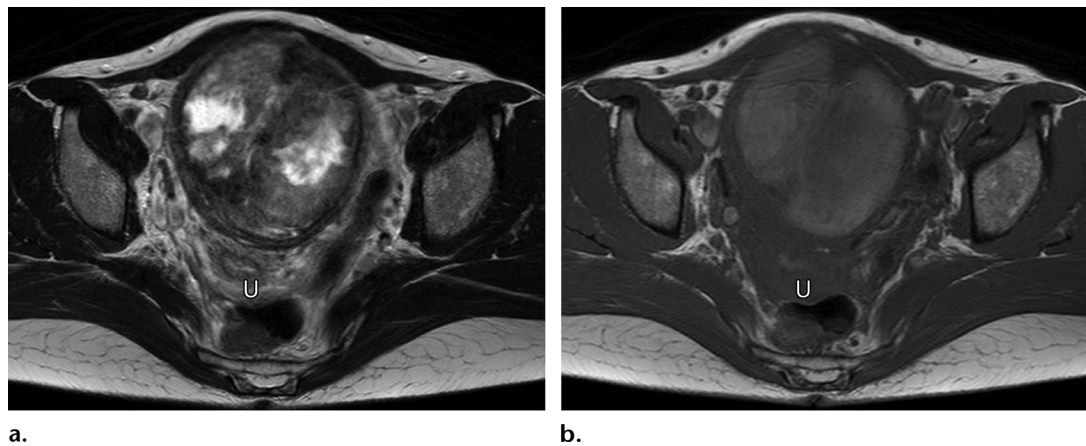
Figure 13.   Red degeneration of leiomyoma in a 31-year-old woman at 14 weeks gestation. *U* = uterus. **(a)** Axial T2-weighted MR image shows a large myoma with a low-intensity rim. **(b)** Axial T1-weighted MR image shows diffuse high intensity within the myoma.

ally and are usually observed simultaneously. With visualization of normal ovaries, ovarian torsion or an ovarian tumor can be eliminated. CT has sufficient ability for evaluating these findings, especially with the use of multiplanar reformations (Fig 14). MR imaging is helpful to confirm normal ovaries,

which may be occasionally invisible on US or CT images (48,49). It may be difficult to identify a twisted pedicle of a subserosal leiomyoma at radiologic imaging because a twisted pedicle of subserosal leiomyoma torsion is thin compared with that of ovarian torsion (Fig 14c). The differential
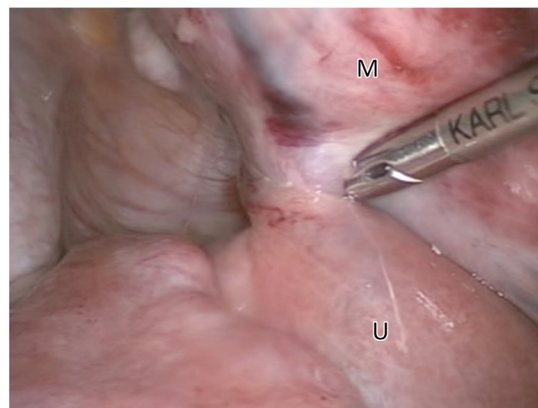
Figure 14. Torsion of a pedunculated subserosal myoma in a 27-year-old woman. (a) Axial contrast-enhanced CT image shows a nonenhanced solid mass (arrow) anterior to the uterus. The ovaries (arrowheads) are normal bilaterally. (b) Sagittal contrast-enhanced CT image shows distortion of the anterior uterine wall (arrowhead), suggestive of a twisted stalk attachment. (c) Intraoperative photograph shows a small twisted pedicle. Note the difference from ovarian torsion as shown in Figure 4d. M = myoma, U = uterus.
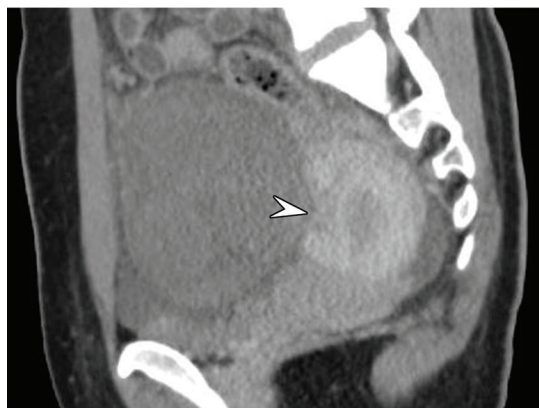
Figure 15. Torsion of a right ovarian dysgerminoma in a 27-year-old woman. (a) Sagittal contrast-enhanced CT image shows a large solid mass (arrow) anterior to the uterus with minimal enhancement that was possibly misinterpreted as torsion of a subserosal myoma. (b) Axial contrast-enhanced CT image during the arterial phase shows a beak-like protrusion (arrowheads) and a right ovarian artery with spiral aspect within the protrusion, indicative of a right ovarian torsion.

diagnosis includes ovarian torsion, especially when the associated ovarian tumor consists of a solid component (Fig 15).

Torsion of the Uterus.—Uterine torsion is an extremely rare condition and is defined as a rotation of the uterus greater than 45° along the long axis (50–55). Uterine torsion is thought to usually occur at the level of the uterine isthmus, the transition between the corpus and cervix. Predisposing factors for uterine torsion include a gravid uterus, a myomatous uterus, congenital uterine anomalies, pelvic adhesions, and adnexal masses. Uterine leiomyomas are the most common pre-
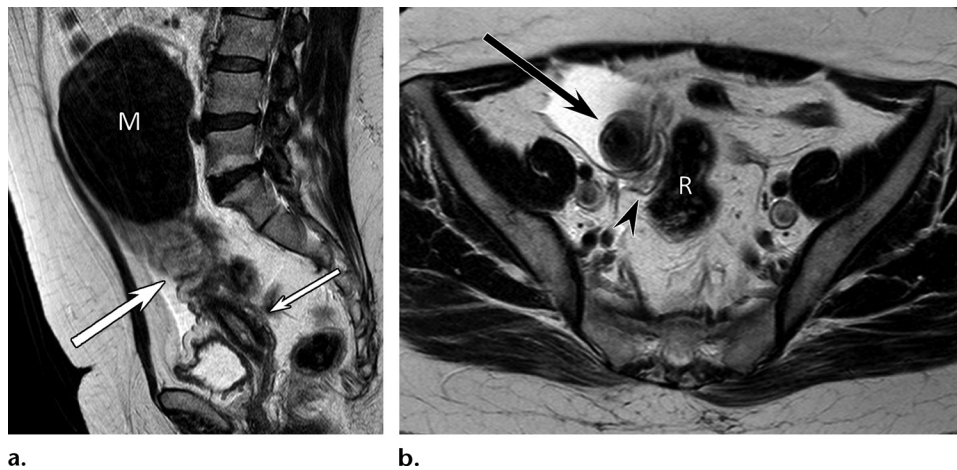
Figure 16. Torsion of the uterus in a 57-year-old woman. **(a)** Sagittal T2-weighted MR image shows a large sessile myoma *(M)* on the uterine fundus. The uterine corpus (large arrow) is obscured, and the uterine cervix (small arrow) is extended. **(b)** Axial T2-weighted MR image at the level of the uterine corpus shows a whirlpool sign (arrow) of a twisted pedicle between the myoma and the cervix, involving the ovaries bilaterally (arrowhead = right ovary). The left ovary is not shown. The uterine corpus was twisted two times. Pathologic analysis confirmed myoma without necrotic change. *R* = rectum.

disposing factor in the case of uterine torsion in a nongravid uterus (Fig 16a).

The clinical presentation of uterine torsion varies from nonspecific mild abdominal discomfort to acute abdominal pain with shock. Preoperative diagnosis is difficult due to its rarity and nonspecific symptoms. An abnormal position of ovarian vessels across the uterus using color Doppler US may help diagnose uterine torsion because bilateral ovaries may be involved in the twisted pedicle, with the broad ligament wrapped around the uterine corpus. The whorled structure of the uterine cervix has been noted on CT scans (52,54). T2-weighted images may also demonstrate the whirlpool sign of the twisted pedicle at the level of the uterine isthmus at MR imaging (Fig 16b).

In our case, the ovaries were obscured bilaterally and appeared to be extended on axial T2-weighted images. One report suggested that an X-shaped configuration of the upper vagina at axial MR imaging led to the preoperative diagnosis of uterine torsion (51); however, the sign may depend on the degree and the level of torsion, as well as the predisposing factors. An accurate diagnosis can be made preoperatively using CT and MR imaging with proper image interpretation and knowledge of this condition.

Acute Uterine Bleeding

Retained products of conception (RPOC) are a common cause of delayed PPH. A uterine arteriovenous malformation (AVM) may also be a cause of delayed PPH, but it is relatively rare. Both RPOC and uterine AVMs have similar clinical manifestations and should be included in the differential diagnosis. Both CT and MR imaging play a supplementary role in the diagnosis of PPH.

RPOC Findings.—RPOC are defined as a persistence of placental tissue in the uterus following delivery or an abortion (56). RPOC occur most frequently after first- and second-trimester delivery or termination of the pregnancy. The symptoms of RPOC include vaginal bleeding and pelvic pain, in some cases. RPOC appear as a mass with various vascularity in the endometrium to the myometrial interface. Color Doppler US allows confident diagnosis of RPOC as an endometrial mass with detectable vascularity. The risk of severe bleeding depends on the depth of invasion into the myometrium and the vascularity of the mass (6). Contrast-enhanced dynamic MR imaging may support the US findings about these factors. MR imaging typically shows an endometrial polypoid mass with heterogeneous signal intensity on T1- and T2-weighted images and variable enhancement on postcontrast images (Fig 17).

The signal intensity of RPOC may vary depending on the degree of hemorrhage, tissue necrosis, and vascularity. Contrast-enhanced dynamic CT is also useful for evaluating the vascularity of the endometrial mass and defining the vascular anatomy before uterine artery embolization. In the case of hypervascular RPOC, CT images show an intensely enhanced mass in the uterine cavity during the early phase, but precise localization of the lesion is somewhat vague compared with that at MR imaging.

RPOC with marked vascularity may mimic a uterine AVM. True uterine AVMs are rare and should persist after RPOC have been excluded

Figure 17. RPOC in a 33-year-old woman. **(a)** Sagittal T2-weighted MR image shows a hyperintense polypoid mass (arrow) in the endometrial cavity and a hypointense area around the mass. **(b)** Sagittal contrast-enhanced T1-weighted MR image shows marked enhancement of the mass (arrow) protruding into the endometrial cavity. **(c)** Right internal iliac arteriogram shows a dilated right uterine artery (arrow) and a hypervascular mass (arrowhead). Bilateral uterine artery embolization was performed before hysteroscopic resection, which confirmed the diagnosis.
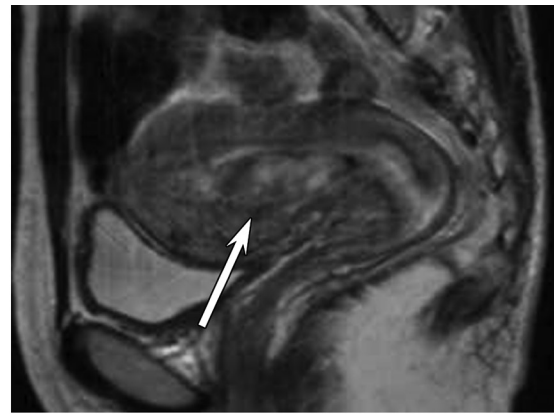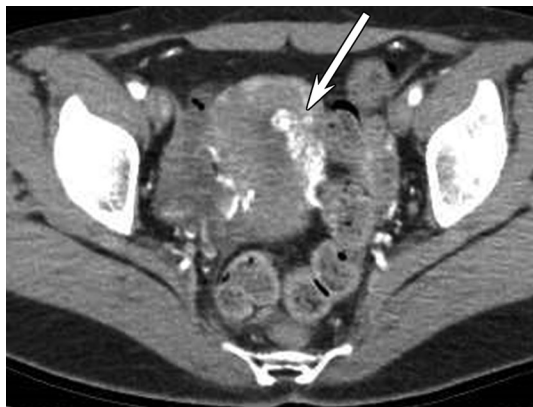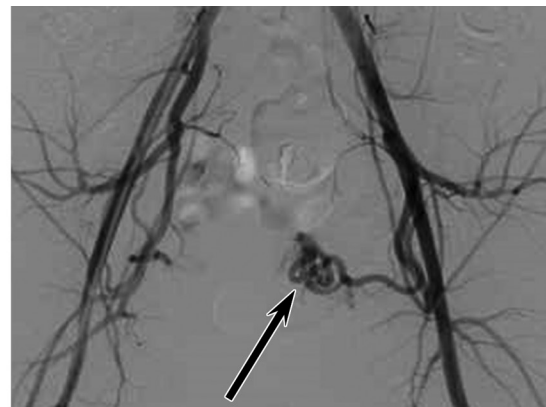

a.

b.
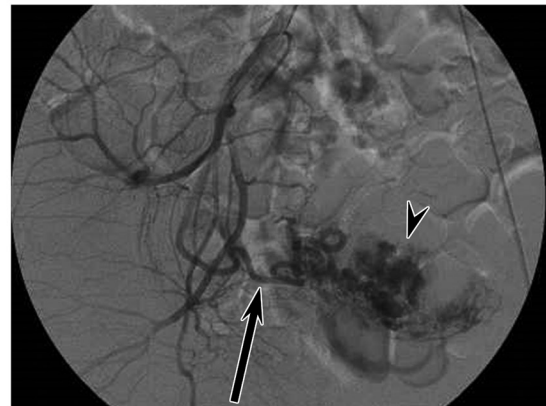
c.

a.

b.

Figure 18.   Presumed diagnosis of a uterine AVM in a 30-year-old patient. **(a)** Axial contrast-enhanced CT image shows a hypervascular mass (arrow) in the endometrial cavity, extending to the myometrium. **(b)** Pelvic angiogram shows a dilated and tortuous left uterine artery (arrow). Early venous return was observed on a delayed image (not shown).

(57). Hypervascular RPOC may cause massive bleeding similar to uterine AVMs (58), and uterine arterial embolization might be selected to control the bleeding before dilation and curettage (59).

Uterine AVMs.—A uterine hypervascular lesion that does not undergo spontaneous regression in a patient with a negative human chorionic

gonadotropin (β-hCG) level is likely an AVM (60). The standard for an AVM diagnosis is early venous return at angiography and myometrial involvement (Fig 18). CT during the arterial phase may show an intensely enhanced structure in the myometrium with extension to the endometrium. MR imaging may show tortuous and tubular signal voids in the myometrium protruding into the endometrial cavity on both T1- and T2-weighted

images. Angiography and embolization are effective in defining the vascular anatomy and treating uterine AVMs.

Although arteriovenous shunting is a typical feature of AVMs, the presence of arteriovenous shunting within the uterine mass does not imply the presence of an AVM (61). The most common cause of myometrial hypervascularity is the persistence of vascular changes in the spiral arteries induced by trophoblastic invasion during pregnancy, which most likely results from RPOC or molar pregnancy (62). This shunting is thought to result from the development of arteriovenous fistulas within the placenta caused by necrosis of the chorionic villi.

Conclusion

CT and MR imaging are helpful in gynecologic emergencies, especially when US findings are indeterminate. CT is ideal for emergency use and can demonstrate internal bleeding, such as hemoperitoneum. CT also allows easy detection of pelvic mass lesions and a presumed diagnosis of a gynecologic emergency; however, CT findings are occasionally nonspecific and may lead to misinterpretation. MR imaging can narrow the differential diagnosis, particularly when adnexal masses or uterine leiomyomas are related to the conditions. Radiologists play an important role in diagnosing acute gynecologic diseases for appropriate treatment.

References

1. Marin D, Boll DT, Mileto A, Nelson RC. State of the art: dual-energy CT of the abdomen. Radiology 2014;271(2): 327–342.
2. Aran S, Daftari Besheli L, Karcaaltincaba M, Gupta R, Flores EJ, Abujudeh HH. Applications of dual-energy CT in emergency radiology. AJR Am J Roentgenol 2014;202(4):W314–W324.
3. Bennett GL, Slywotzky CM, Giovanniello G. Gynecologic causes of acute pelvic pain: spectrum of CT findings. RadioGraphics 2002;22(4):785–801.
4. Kim JH, Lee SM, Lee JH, et al. Successful conservative management of ruptured ovarian cysts with hemoperitoneum in healthy women. PLoS One 2014;9(3):e91171.
5. Potter AW, Chandrasekhar CA. US and CT evaluation of acute pelvic pain of gynecologic origin in nonpregnant premenopausal patients. RadioGraphics 2008;28(6): 1645–1659.
6. Dohke M, Watanabe Y, Okumura A, et al. Comprehensive MR imaging of acute gynecologic diseases. RadioGraphics 2000;20(6):1551–1566.
7. Kanso HN, Hachem K, Aoun NJ, et al. Variable MR findings in ovarian functional hemorrhagic cysts. J Magn Reson Imaging 2006;24(2):356–361.
8. Kao LY, Scheinfeld MH, Chernyak V, Rozenblit AM, Oh S, Dym RJ. Beyond ultrasound: CT and MRI of ectopic pregnancy. AJR Am J Roentgenol 2014;202(4):904–911.
9. Chang HC, Bhatt S, Dogra VS. Pearls and pitfalls in diagnosis of ovarian torsion. RadioGraphics 2008;28(5):1355–1368.
10. Lourenco AP, Swenson D, Tubbs RJ, Lazarus E. Ovarian and tubal torsion: imaging findings on US, CT, and MRI. Emerg Radiol 2014;21(2):179–187.
11. Duigenan S, Oliva E, Lee SI. Ovarian torsion: diagnostic features on CT and MRI with pathologic correlation. AJR Am J Roentgenol 2012;198(2):W122–W131.
12. Rha SE, Byun JY, Jung SE, et al. CT and MR imaging features of adnexal torsion. RadioGraphics 2002;22(2):283–294.
13. Patil AR, Nandikoor S, Rao A, et al. Multimodality imaging in adnexal torsion. J Med Imaging Radiat Oncol 2015;59(1):7–19.
14. Fujii S, Kaneda S, Kakite S, et al. Diffusion-weighted imaging findings of adnexal torsion: initial results. Eur J Radiol 2011;77(2):330–334.
15. Kato H, Kanematsu M, Uchiyama M, Yano R, Furui T, Morishige K. Diffusion-weighted imaging of ovarian torsion: usefulness of apparent diffusion coefficient (ADC) values for the detection of hemorrhagic infarction. Magn Reson Med Sci 2014;13(1):39–44.
16. Kilickesmez O, Tasdelen N, Yetimoglu B, Kayhan A, Cihangiroglu M, Gurmen N. Diffusion-weighted imaging of adnexal torsion. Emerg Radiol 2009;16(5):399–401.
17. Moribata Y, Kido A, Yamaoka T, et al. MR imaging findings of ovarian torsion correlate with pathological hemorrhagic infarction. J Obstet Gynaecol Res 2015;41(9):1433–1439.
18. Praveen R, Pallavi V, Rajashekar K, Usha A, Umadevi K, Bafna U. A clinical update on massive ovarian oedema: a pseudotumour? Ecancermedicalscience 2013;7(1):318.
19. Lee AR, Kim KH, Lee BH, Chin SY. Massive edema of the ovary: imaging findings. AJR Am J Roentgenol 1993;161(2): 343–344.
20. Chiou SY, Lev-Toaff AS, Masuda E, Feld RI, Bergin D. Adnexal torsion: new clinical and imaging observations by sonography, computed tomography, and magnetic resonance imaging. J Ultrasound Med 2007;26(10):1289–1301.
21. Yamashiro T, Inamine M, Kamiya H, Kinjo A, Murayama S, Aoki Y. Massive ovarian edema with torsion: unusual hemorrhage and the recovery of contrast enhancement. Emerg Radiol 2008;15(2):115–118.
22. Geist RR, Rabinowitz R, Zuckerman B, et al. Massive edema of the ovary: a case report and review of the pertinent literature. J Pediatr Adolesc Gynecol 2005;18(4):281–284.
23. Cheng MH, Tseng JY, Suen JH, Yang CC. Laparoscopic plication of partially twisted ovary with massive ovarian edema. J Chin Med Assoc 2006;69(5):236–239.
24. Lo LM, Chang SD, Lee CL, Liang CC. Clinical manifestations in women with isolated fallopian tubal torsion: a rare but important entity. Aust N Z J Obstet Gynaecol 2011;51(3):244–247.
25. Vijayaraghavan SB, Senthil S. Isolated torsion of the fallopian tube: the sonographic whirlpool sign. J Ultrasound Med 2009;28(5):657–662.
26. Harmon JC, Binkovitz LA, Binkovitz LE. Isolated fallopian tube torsion: sonographic and CT features. Pediatr Radiol 2008;38(2):175–179.
27. Casey RK, Damle LF, Gomez-Lobo V. Isolated fallopian tube torsion in pediatric and adolescent females: a retrospective review of 15 cases at a single institution. J Pediatr Adolesc Gynecol 2013;26(3):189–192.
28. Toyoshima M, Mori H, Kudo K, et al. Isolated torsion of the fallopian tube in a menopausal woman and a pre-pubertal girl: two case reports. J Med Case Reports 2015;9:258.
29. Rezvani M, Shaaban AM. Fallopian tube disease in the nonpregnant patient. RadioGraphics 2011;31(2): 527–548.
30. Gross M, Blumstein SL, Chow LC. Isolated fallopian tube torsion: a rare twist on a common theme. AJR Am J Roentgenol 2005;185(6):1590–1592.
31. Kiseli M, Caglar GS, Cengiz SD, Karadag D, Yılmaz MB. Clinical diagnosis and complications of paratubal cysts: review of the literature and report of uncommon presentations. Arch Gynecol Obstet 2012;285(6):1563–1569.
32. Yilmaz Y, Ozen IO, Caliskan D, Dilmen U. Paraovarian cyst torsion in children: report of two cases. Pediatr Int 2013;55(6):795–797.

33. Fibus TF. Intraperitoneal rupture of a benign cystic ovarian teratoma: findings at CT and MR imaging. AJR Am J Roentgenol 2000;174(1):261–262.

34. Ayhan A, Bukulmez O, Genc C, Karamursel BS, Ayhan A. Mature cystic teratomas of the ovary: case series from one institution over 34 years. Eur J Obstet Gynecol Reprod Biol 2000;88(2):153–157.

35. Hosokawa T, Sato Y, Seki T, Maebara M, Ito K, Kuribayashi S. Malignant transformation of a mature cystic teratoma of the ovary with rupture. Jpn J Radiol 2010;28(5):372–375.

36. Dai X, Jin C, Hu Y, et al. High CA-125 and CA19-9 levels in spontaneous ruptured ovarian endometriomas. Clin Chim Acta 2015;450:362–365.

37. Lee YR. CT imaging findings of ruptured ovarian endometriotic cysts: emphasis on the differential diagnosis with ruptured ovarian functional cysts. Korean J Radiol 2011;12(1):59–65.

38. Kurata H, Sasaki M, Kase H, Yamamoto Y, Aoki Y, Tanaka K. Elevated serum CA125 and CA19-9 due to the spontaneous rupture of ovarian endometrioma. Eur J Obstet Gynecol Reprod Biol 2002;105(1):75–76.

39. Corwin MT, Gerscovich EO, Lamba R, Wilson M, McGahan JP. Differentiation of ovarian endometriomas from hemorrhagic cysts at MR imaging: utility of the T2 dark spot sign. Radiology 2014;271(1):126–132.

40. Kim SH, Kim SH, Yang DM, Kim KA. Unusual causes of tubo-ovarian abscess: CT and MR imaging findings. RadioGraphics 2004;24(6):1575–1589.

41. Ha HK, Lim GY, Cha ES, et al. MR imaging of tubo-ovarian abscess. Acta Radiol 1995;36(5):510–514.

42. Sam JW, Jacobs JE, Birnbaum BA. Spectrum of CT findings in acute pyogenic pelvic inflammatory disease. RadioGraphics 2002;22(6):1327–1334.

43. Koh DM, Collins DJ. Diffusion-weighted MRI in the body: applications and challenges in oncology. AJR Am J Roentgenol 2007;188(6):1622–1635.

44. Ueda H, Togashi K, Konishi I, et al. Unusual appearances of uterine leiomyomas: MR imaging findings and their histopathologic backgrounds. RadioGraphics 1999;19(Spec Issue):S131–S145.

45. Roche O, Chavan N, Aquilina J, Rockall A. Radiological appearances of gynaecological emergencies. Insights Imaging 2012;3(3):265–275.

46. Kawakami S, Togashi K, Konishi I, et al. Red degeneration of uterine leiomyoma: MR appearance. J Comput Assist Tomogr 1994;18(6):925–928.

47. Roy C, Bierry G, El Ghali S, Buy X, Rossini A. Acute torsion of uterine leiomyoma: CT features. Abdom Imaging 2005;30(1):120–123.

48. Marcotte-Bloch C, Novellas S, Buratti MS, Caramella T, Chevallier P, Bruneton JN. Torsion of a uterine leiomyoma: MRI features. Clin Imaging 2007;31(5):360–362.

49. Gupta S, Manyonda IT. Acute complications of fibroids. Best Pract Res Clin Obstet Gynaecol 2009;23(5):609–617.

50. Matsumoto H, Ohta T, Nakahara K, Kojimahara T, Kurachi H. Torsion of a nongravid uterus with a large ovarian cyst: usefulness of contrast MR image. Gynecol Obstet Invest 2007;63(3):163–165.

51. Nicholson WK, Coulson CC, McCoy MC, Semelka RC. Pelvic magnetic resonance imaging in the evaluation of uterine torsion. Obstet Gynecol 1995;85(1, pt 2):888–890.

52. Jeong YY, Kang HK, Park JG, Choi HS. CT features of uterine torsion. Eur Radiol 2003;13(suppl 6):L249–L250.

53. Sharma D, Usha M. Torsion of a non-gravid uterus: a rare cause of acute abdomen. Int J Reprod Contracept Obstet Gynecol 2013;2(2):234–236.

54. Luk SY, Leung JL, Cheung ML, So S, Fung SH, Cheng SC. Torsion of a nongravid myomatous uterus: radiological features and literature review. Hong Kong Med J 2010;16(4):304–306.

55. Hawes CH. Acute axial torsion of the uterus. Ann Surg 1935;102(1):37–40.

56. Sellmyer MA, Desser TS, Maturen KE, Jeffrey RB Jr, Kamaya A. Physiologic, histologic, and imaging features of retained products of conception. RadioGraphics 2013;33(3):781–796.

57. Kamaya A, Petrovitch I, Chen B, Frederick CE, Jeffrey RB. Retained products of conception: spectrum of color Doppler findings. J Ultrasound Med 2009;28(8):1031–1041.

58. Kido A, Togashi K, Koyama T, et al. Retained products of conception masquerading as acquired arteriovenous malformation. J Comput Assist Tomogr 2003;27(1):88–92.

59. Kitahara T, Sato Y, Kakui K, Tatsumi K, Fujiwara H, Konishi I. Management of retained products of conception with marked vascularity. J Obstet Gynecol Res 2011;37(5):458–464.

60. Cura M, Martinez N, Cura A, Dalsaso TJ, Elmerhi F. Arteriovenous malformations of the uterus. Acta Radiol 2009;50(7):823–829.

61. Huang MW, Muradali D, Thurston WA, Burns PN, Wilson SR. Uterine arteriovenous malformations: gray-scale and Doppler US features with MR imaging correlation. Radiology 1998;206(1):115–123.

62. Müngen E, Dundar O, Babacan A. Postabortion Doppler evaluation of the uterus: incidence and causes of myometrial hypervascularity. J Ultrasound Med 2009;28(8):1053–1060.